First flux-penetration fields in $L_{2-x}Ce_xCuO_{4-y}$ single crystals

L. Fàbrega, J. Fontcuberta, B. Martínez, and S. Piñol
Institut de Ciència de Materials de Barcelona, Consejo Superior de Investigaciones Científicas, Campus de la Universidat Autònoma de Barcelona, 08193 Bellaterra, Catalunya, Spain
(Received 21 December 1993)

High-resolution measurements of low-field dc magnetization are used to obtain flux-penetration fields $H_p(T)$ along the two main crystallographic directions of several $L_{2-x}Ce_xCuO_{4-y}$ (L=Pr,Nd,Sm) single crystals. The departure from the linearity of the virgin $M(H)$ curve and the appearance of remanence and magnetic relaxation are used to determine H_p. It is shown that $H_p(T)$ may not be safely identified with $H_{c1}(T)$ when $\mathbf{H}\|c$; the implications of these results are discussed in order to estimate the values of the fundamental superconducting quantities as the lower critical field, the penetration depth, the Ginzburg-Landau parameter, and the anisotropy in these electron-doped copper oxide superconductors.

INTRODUCTION

One of the most important parameters of type-II superconductors is the lower critical field H_{c1}. Its values along the main directions in anisotropic superconductors allow one to estimate the penetration depths of a magnetic field and thus may provide the anisotropy ratio Γ of the material; furthermore, the ratio H_{c2}/H_{c1} provides estimates of the Ginzburg-Landau parameter κ. Γ and κ are of fundamental interest in order to evaluate the elasticity of the flux-line lattice in the mixed state, and consequently the maximum pinning force a particular kind of defect can exert on the vortices.

H_{c1} is defined as the field at which the nucleation of a vortex inside the superconductor becomes energetically favorable; as a consequence, it is usually assumed that this field corresponds to the boundary between the Meissner and the mixed states in the H-T phase diagram. Hence, a common experimental way to determine $H_{c1}(T)$ turned out to be its identification with the lowest field at which flux penetration is observed, $H_p(T)$.

Flux penetration may be identified in the low-field $M(H)$ curves as a deviation from the linear $M=-H$ behavior corresponding to the Meissner state. Other signatures of the departure from the total screening are related to the existence of flux pinning: once vortices are present inside the sample, the superconductor enters an irreversible state, and phenomena as magnetic relaxation and remanence may appear. One might thus conclude that $H_{c1}(T)$ is experimentally well defined.

However, due to the finite size of samples and thus the existence of boundaries, in real samples the first flux penetration is expected to occur at fields $H_p > H_{c1}$. Two reasons, often mixed, stand out for this behavior: first, the existence of surface barriers in samples with perfect surfaces prevents flux from entering up to applied fields of the order of the thermodynamic critical field, $H_p = H_c/\sqrt{2}$;[1] surface roughness[2] and thermal activation[3,4] cause H_p to be lower, that is, $H_{c1} < H_p < H_c/\sqrt{2}$. Second, flux pinning reduces the flux-penetration rate, as pinned vortices near the surface hinder the penetration of new flux lines.[5] A third reason complicating the evaluation of H_{c1} from H_p is related to demagnetizing effects: single crystals of anisotropic materials, such as copper oxides, are usually thin slabs, and consequently an inhomogeneous demagnetizing field, much higher than the external field H_a, appears when H_a is applied perpendicular to the largest surface of the sample. The evaluation of this field is a hard issue when the magnetization is inhomogeneous, i.e., in irreversible states.[6,7]

Consequently, it is not obvious at all how the experimental determination of $H_p(T)$ can provide information regarding the intrinsic parameters of the superconductor. Indeed, the $H_{c1}(T)$ values obtained for high-temperature superconductors (HTSC) from flux-penetration criteria are usually sample dependent[2,4,8] and do not display the expected behavior from mean-field theories. This effect is particularly important in the electron-doped copper oxides $L_{2-x}Ce_xCuO_{4-y}$ (LCCO); the scarce reported values for H_{c1}^c range between 2.65 mT (Ref. 9) and 0.2 T.[10] Although estimates for H_{c2}^c and ξ_{ab} are already available, the scattered values of the lower critical field do not allow one to obtain accurate estimates of parameters as important as κ and Γ, which are nowadays the most controversial issues in these materials. The problem is even enhanced by the fact that the direct measurement of the London penetration depth along the *ab* planes λ_{ab} (corresponding to $H_a\|c$) by, for instance, μSR techniques, is hindered by the magnetic moment of the rare-earth ions L^{3+} in this system.[11]

In this paper we perform a detailed analysis of the nature of first flux penetration in several $L_{2-x}Ce_xCuO_{4-y}$ (L=Pr,Nd,Sm) single crystals, along the two main crystallographic directions. The effects of surface barriers, pinning, and extreme shape are examined; limits to the actual H_{c1}^c and H_{c1}^{ab} values, as well as estimates for the penetration depths along the *c* axis and the *ab* planes, $\lambda_c(0)$ and $\lambda_{ab}(0)$, are obtained.

EXPERIMENT

The first flux-penetration field H_p along the **c** axis and the **ab** planes of several $L_{2-x}Ce_xCuO_{4-y}$ (L=Nd,Pr,Sm) single crystals has been obtained from low-field magneti-

zation $M(H,T,t)$ measurements ($\mu_0 H_a \leq 20$ mT, $T \geq 2$ K, $\Delta t \leq 45$ min), by using a commercial superconducting quantum interference device (SQUID) magnetometer.

The studied single crystals were grown by the self-flux method;[12] they are thin platelets with the largest surface S perpendicular to the c-axis direction. Their mass m and dimensions are displayed in Table I. $\varepsilon \equiv V/S$ is their thickness; V is the volume, evaluated from the mass and the theoretical density of the material; due to the irregular shape of the surface S of the crystals, this method has been found to be more reliable than the determination of the volume from the main dimensions of the samples; $a \equiv \sqrt{S/\pi}$ is the effective radius of the samples. Also displayed in Table I are the critical temperature T_c and the transition width ΔT_c of the crystals, evaluated from the low-field ($\mu_0 H_a \approx 10^{-4}$ T) zero-field-cooling (ZFC) transition when $\mathbf{H_a} \| \mathbf{c}$.

Magnetization measurements in the SQUID magnetometer were carried out by using a scan length of 3 cm, to avoid effects of field inhomogeneity. Measurements were found to be completely reproducible for scan lengths ranging between 1.5 and 3 cm. The magnetization M per unit volume was obtained from the volume V. Before each low-field measurement, the remanent field in the superconducting coil was reduced to a value of the order of $\mu_0 H_{rem} \approx 10^{-5}$ T by applying fields of progressively reduced value and alternate polarity. After this process, H_{rem} was carefully determined by using a Pb test sample, and conveniently taken into account in the subsequent measuring sequences.

Due to the small order of magnitude of the superconducting signal for $\mathbf{H_a} \| \mathbf{ab}$, the magnetization measurements in this direction were carried out by using a quartz fiber sample holder,[13] with the aim of (i) obtaining a good orientation between the external field H_a and the **ab** planes of the crystals, and (ii) minimizing the sample holder contribution. In view of the low H_p values along this direction ($\mu_0 H_p^{ab} \sim 10^{-4}$ T), the external field was applied by using the superconducting coil of the commercial SQUID magnetometer and substituting the power supply of the equipment by a high stability external power supply ($\Delta H_a / H_a < 0.05\%$ for $\mu_0 H_a \leq 15$ mT).

The demagnetizing factor N in the $\mathbf{H_a} \| \mathbf{c}$ direction has been experimentally determined by means of the slope of the low-field linear magnetization and the relation $dM/dH_a = -1/(1-N)$;[6] in the calculation of the initial slope of $M(H_a)$ care has been taken in order to ensure that the H_a fields used do not exceed the first flux-penetration field later obtained, that is, $H_a < (1-N)H_p$. Table I summarizes the N values obtained for the analyzed single crystals by using this method, as well as a theoretical estimate, N_{calc}, corresponding to the demagnetizing factor of a disk of radius $a \equiv \sqrt{S/\pi}$ and length $\varepsilon \ll a$.[14] It may be noticed that $1-N \ll 1$ in all cases, in accordance with the extreme sample shape. Although there is a clear correlation between N and N_{calc}, the difference between both values increases as the crystals become thicker. This increasing difference may be related to the fact that the expression used to compute N_{calc} is expected to hold for $\varepsilon \ll a$; Obviously, this limit is progressively left as crystals become thicker. In general, $N_{calc} < N$; this is likely due to corner effects: in these zones the density of flux lines is higher than the estimated for the ideal disk-shaped samples considered in Ref. 14, and consequently the average internal field H is higher than that obtained from the theoretical calculation N_{calc}. Due to these considerations, we believe that the measured N values allow a better evaluation of the average demagnetizing field than N_{calc}, and we will use them in the analysis of our data.

In the $\mathbf{H_a} \| \mathbf{ab}$ configuration, the misorientation between the applied field and the **ab** plane of the crystal has been estimated to be $\Delta\theta \leq 0.3°$ from measurements of the angular dependence of the transverse magnetization; it is important to stress that this misorientation, which would be very important in the measurement of some anisotropic superconducting properties, is not relevant in the case of $H_{c1}(T)$, as $H_{c1}^c \gg H_{c1}^{ab}$; indeed, the effective field along the c-axis direction is $H \| c \approx H_a \sin(\Delta\vartheta)/(1-N) < 0.2 H_a$ and consequently the first flux penetration would always correspond to the $\mathbf{H} \| \mathbf{ab}$ contribution.

TABLE I. Characteristics of the $L_{1.85}Ce_{0.15}CuO_{4-y}$ single crystals analyzed in this work.

Name	L	T_c (K)	ΔT_c (K)	m (mm)	a (mm)	ε (μm)	N	N_{calc}
Pr1	Pr	19.2	1.5	0.43	0.79	30	0.946	0.940
Pr2	Pr	16.5	3.0	0.786	0.76	59	0.917	0.878
Pr3	Pr	21.0	5.0	1.374	0.86	81	0.923	0.851
Pr4	Pr	18.0	2.0	0.458	0.57	61	0.868	0.832
Nd1	Nd	25.5	4.0	0.510	0.98	23	0.969	0.963
Nd2	Nd	23.0	2.5	0.210	0.60	25	0.955	0.934
Sm1	Sm	23.0	4.0	0.726	0.66	72	0.895	0.827

RESULTS

A. H||c

Figure 1 displays the first magnetization curves, as a function of the applied magnetic field $H_a \| \mathbf{c}$, at several

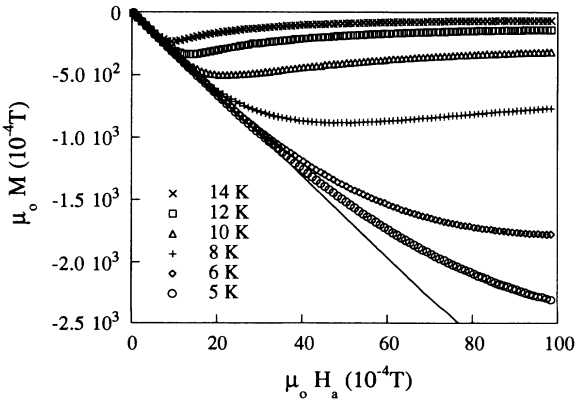

FIG. 1. First magnetization curves at several temperatures, in crystal Nd1. The line corresponds to the Meissner magnetization; it has been obtained from the low-field data measured at the lowest temperature.

temperatures, for crystal Nd1. The shape of the $M(H_a)$ curve, its temperature dependence, and the H_a field range where flux penetration appears are similar for all measured crystals.

The first flux penetration can be more accurately determined[15,16] by subtracting the Meissner magnetization $M=-H$ to the measured signal. Here H is the average internal field corresponding to the applied field H_a and the measured average magnetization M; it can be obtained from the expression[6]

$$H=H_a-NM \ . \tag{1}$$

Equivalently, one may evaluate the average flux density inside the sample, $B=\mu_0(H+M)$, which should be zero in the Meissner state. Figure 2, displaying $B(H)$ in crystal Nd1 at several temperatures, reveals that flux penetration appears suddenly at high temperatures and turns smoother at lower temperatures. This slowing down of the penetration rate may be due to either a more effective flux pinning or a reduction of the overcome of surface barriers by thermal activation. The slight backwards curvature of the $B(H)$ curves measured at the highest temperatures is simply related to the inaccuracy of the demagnetizing field correction, Eq. (1), when flux gradients within the crystal may not be ignored (see below).

The field H_p at which the first flux penetration occurs may be determined by two different methods: (a) from the lowest field producing a B value above a fixed threshold $B_{\rm res}$, or (b) from the extrapolation towards $B=0$ of the region where flux has already penetrated the sample. The first method, besides the arbitrariness of the $B_{\rm res}$ choice, may be affected by the rounding of $B(H)$ caused by shape effects (higher flux density in corners, etc.). The second method, commonly used,[15] introduces two problems: (i) it requires the presumption of a model for flux penetration; the Bean model[17] is regularly assumed to hold, which predicts

$$B\sim(H-H_p)^2 \tag{2}$$

for partial penetration ($H_p<H<H_1^*$, where H_1^* is the full penetration field in the critical state model). (ii) Eq. (1) is not suitable to account for the demagnetizing field when the sample is in a state of magnetic irreversibility,[6] i.e., at any field above H_p; if H is not properly evaluated, the $B=0$ extrapolation provides incorrect H_p values, even when the function used to describe $B>0$ might be the appropriate one. Nevertheless, since flux density is usually very small close to $H_p(T)$, flux gradients inside the material are assumed to represent only a small contribution to the overall magnetization M, so that this latter difficulty is considered not to be relevant at low temperature (see below).

Figure 3 displays the square root of B as a function of the internal field H [evaluated by using Eq. (1)], in crystal Nd1. Clearly, the prediction of the Bean model [Eq. (2)] is only fulfilled at the lowest temperatures: as T increases, $\sqrt{B}$ increases with a function faster than linear, thus indicating that the extrapolation to zero of $\sqrt{B}$ cannot be safely used to extract H_p. From the above discussions, several explanations for this failure may be put forward. First, strong field and temperature dependences of the critical current have been reported from magnetic relaxation and hysteresis cycles on LCCO single crystals;[18,19] under these circumstances, Eq. (2), obtained with the assumption of a field-independent critical current, may not hold. Second, the law given by Eq. (2) is not expected to provide a good description of flux penetration in the presence of surface barriers, which are likely to be relevant in high-κ materials.[1,2,4] And third, recently Brandt and co-workers,[20] have pointed out that the Bean model is not suitable to describe flux penetration in thin slabs ($a\gg\varepsilon$), when the applied field is perpendicular to the largest surface; these authors have shown, by the detailed calculation of the current distribution in the case of a critical current constant with field, that in this geometry flux starts penetrating the sample at a field $H_p>H_{c1}$. This result implies that the effect of bulk pinning on the penetration onset is similar to that of a surface barrier. In single crystals of highly anisotropic extreme type-II superconductors, as copper oxides are, both contributions may be significant and difficult to distin-

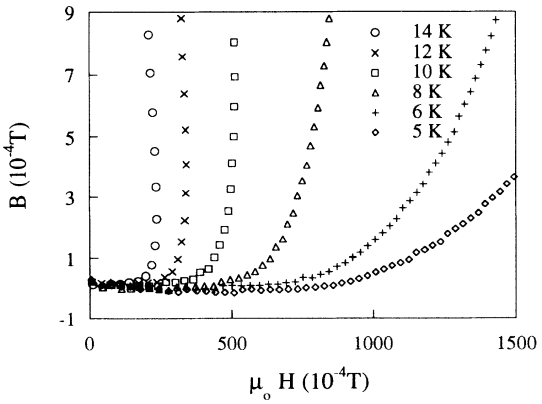

FIG. 2. Deviation from linearity in the first magnetization curve, as a function of the internal field, in crystal Nd1.

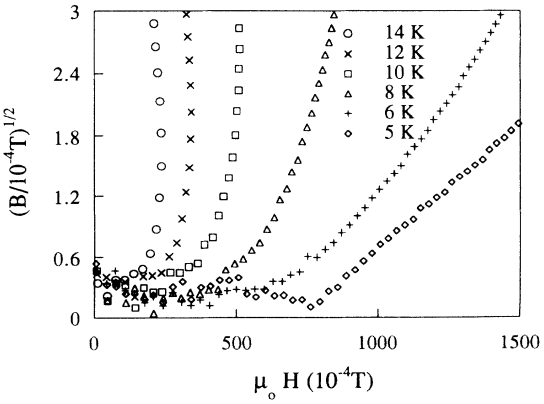

FIG. 3. Square root of magnetic induction inside sample, as a function of the internal magnetic field, in crystal Nd1.

guish.

More information regarding the nature of flux penetration can be gained from the analysis of the remanent magnetization, $M_{rem}(T,H_a)$; in this case, H_p may be identified with the lowest field causing a nonzero value of M_{rem}. Figure 4 displays M_{rem} in crystal Nd2 as a function of the applied field at several temperatures. The measuring procedure is the following: a field $H_a^1=\Delta H_a$ is applied after a zero-field-cooling (ZFC) process down to the desired temperature; after a waiting time Δt ($1s \leq \Delta t \leq 60s$), the field H_a is removed and the magnetization M_{rem} is measured; a new field $H_a^{n+1}=H_a^n+\Delta H_a$ is then applied, and the process is repeated successively. Figure 4(b) shows that the $M_{rem}(H_a)$ behavior is similar to that displayed by the deviation from linearity (Fig. 2): at low T, M_{rem} departs from zero very slowly, and so increases; at high temperatures, remanence appears suddenly and reaches its saturation value in a narrow field range. Within a critical state model, this behavior means that at high temperatures the first penetration field H_p and the full penetration field H_1^* lie close, i.e., flux penetration through the whole sample occurs in a narrow field range; thus, the contribution of the irreversible magnetization to the overall signal may not be ignored near H_p. Consequently, Eq. (1) is not accurate enough to calculate H above $H_p(T)$ at high temperatures; in fact, the backwards curvature of the high-temperature $B(H)$ curves in Fig. 2 results from this inherent difficulty.

On the other hand, it was shown in Refs. 18 and 19 that the critical currents $J_c(T,H)$ in similar LCCO single crystals display an exponential field decay; calculations of $M(H)$ in a critical state model with this field dependence for J_c showed that both H_1^* and the field H_2^* above which $M_{rem}(H)=$const are of the order of the characteristic field of the exponential decay.[21] The low values of H_1^* and H_2^* revealed by Fig. 4(a) are therefore a signature of sharp field decays of J_c. In such a case, the field dependence of J_c may not be ignored, even in the analyzed narrow range of low fields, and thus the Bean expression [Eq. (2)]—obtained under the assumption of a field-independent J_c—should not be suitable in order to describe our data, as already appreciated in Fig. 3.

In fact, comparison between the flux B which has penetrated the sample after applying a field H_a, and the flux remaining inside after removing the external field, $B_{rem}=\mu_0(H+M_{rem})\approx\mu_0(1-N)M_{rem}$, indicates that the use of the Bean model is not suitable at all to describe the present data. Figure 5 displays B and B_{rem} in crystal Nd2 at $T=5$ K. According to the simplest Bean model,[17] it should be $B_{rem}=B/2$ in the field range $H_p<H<H_1^*$; however, as it can be clearly appreciated in our data of Fig. 5, this simple relation does not hold but we have $B_{rem}>B/2$ for any field $H>H_p$. A first possible origin for this discrepancy is the difficulty in evaluating B_{rem}, as Eq. (1), used to estimate H, is not suitable when $H_a=0$ because remanent flux is inhomogeneously distributed inside the sample. From another viewpoint, it has been shown[22] that in a critical state model with a strong $J_c(H)$ dependence the ratio B_{rem}/B is not constant but increases when increasing H, from its minimum value $B_{rem}/B=\frac{1}{2}$ at $H=H_p$. Consequently, our experimental observation of $B_{rem}>B/2$ could be due to a strong-exponential-field decay of the critical current, already discussed and reported in Refs. 18 and 19. Indeed, we have

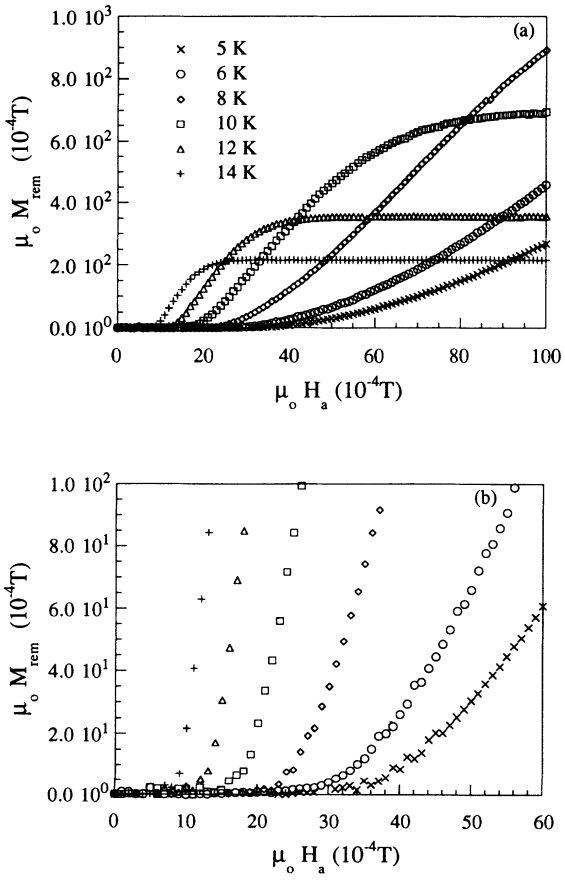

FIG. 4. Remanent magnetization after applying a field H_a, waiting $\Delta t=1$ s and removing H_a, in crystal Nd2, in the whole measured field range (a) and in the region close to $B=0$ (b).

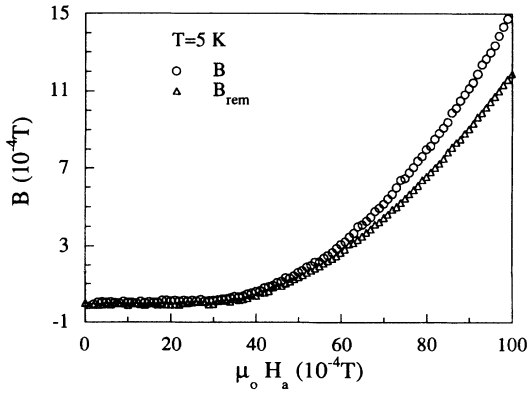

FIG. 5. Penetrated flux B and remanent flux B_{rem} in crystal Nd2, as a function of the applied field H_a, $T=5$ K.

observed that the ratio B_{rem}/B increases for increasing temperatures; this result agrees with the sharpening of the field decay of the critical current at high temperatures [Fig. 4(a)].

On the other hand, the low H_1^* values at high temperatures point to a weak effect of flux pinning (low critical currents), as discussed in Ref. 19; in this case, an important magnetic relaxation—thermally activated overcome of the pinning potential wells—might exist.[23] A first evidence of magnetic relaxation is provided by the analysis of the effect on M_{rem} of the waiting time Δt between the establishment of the applied field H_a and its removal. Figure 6, displaying the isothermal ($T=8$ K) remanence in crystal Nd2 measured with $\Delta t=1$ s and $\Delta t=60$ s, reveals that M_{rem} depends on Δt at any field above $H_p(T)$; this behavior simply reflects that during the time Δt more flux lines penetrate into the crystal and thus more vortices remain pinned after removing the applied field. A consequence of this time dependence of flux penetration is an error in the determination of H_p as the field value where M_{rem} or B extrapolate to zero, no matter which model is used; this effect may be clearly appreciated in Fig. 6.

The time dependence of flux penetration may be due to either a decay of the flux profile inside the material, related to flux jumps over their pinning potential wells,[23] or the overcome of surface barriers by thermal activation.[4] A deeper analysis of the relaxation phenomenon revealed by Fig. 6 may be obtained by recording the time dependence of magnetization at different applied fields, in the vicinity of the flux penetration onset. Figures 7(a)–7(d) display magnetization at $T=10$ K in crystal Nd2 after a ZFC, as a function of time at four different applied fields, $\mu_0 H_a=1.2$, 1.4, 1.6, and 1.8 mT, respectively; the time decay of M has been recorded during 45 min for each field. M does not depend on time at the lowest fields [Figs. 7(a) and 7(b)], as expected in a reversible (Meissner, i.e., $B=0$) regime. Relaxation becomes suddenly apparent at a certain field value, $\mu_0 H_a=1.6$ mT [Fig. 7(c)]; a slight increase of H_a, of 0.2 mT [Fig. 7(d)], duplicates the magnetization decay. This strong field dependence of the relaxation rate may allow us to distinguish between thermal activation over the surface barriers and relaxation of the flux profile inside the crystal. Indeed, Koshelev[24] estimated the field dependence of the surface barrier height U_s and showed that for $B\approx 0$ (flux penetration onset) it is $U_s\sim\ln(H)$; this author argued that,

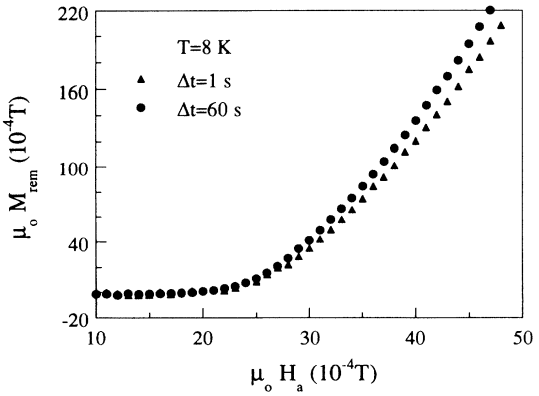

FIG. 6. Remanence at $T=8$ K in crystal Nd2. Influence of the waiting time Δt before removing the applied field H_a.

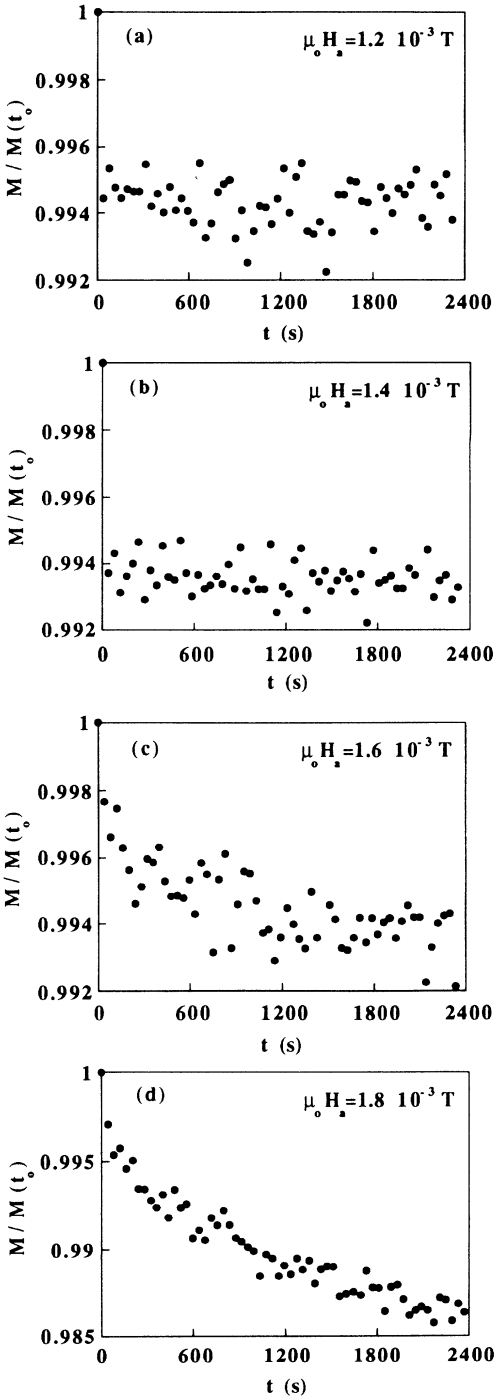

FIG. 7. Time decays of magnetization at $T=10$ K in crystal Nd2, for applied fields $\mu_0 H_a=1.2$ (a), 1.4 (b), 1.6 (c), and 1.8×10^{-3} T (d). Magnetic relaxation appears suddenly at $\mu_0 H_a=1.6\times10^{-3}$ T.

though surface defects may change the absolute value of U_s, they should not modify its field dependence. A smooth field dependence of the relevant activation barriers, as the logarithmic one expected for U_s, cannot account for the strong field dependence of the relaxation rate revealed by Figs. 7(c) and 7(d). We should thus conclude that the magnetization decay observed in our data is related to flux motion between different pinning potential wells in the bulk material.

As the superconductor is in a nonequilibrium state for $H > H_p$, M should be expected to decay with time. If thermally activated flux motion is important, as argued above, this time decay should be apparent at any field above H_p (see also Fig. 6). We will thus identify $H_p(T)$ with the field causing the first magnetization decay.

Figure 8 summarizes the first flux-penetration fields in crystal Nd2, obtained by the four different procedures discussed, namely from (i) and (ii) the deviation from the linear $M=-H$ behavior (by using either a $B_{res}=2\times10^{-5}$ T criterion and the linear extrapolation towards $B=0$ of $\sqrt{B}$), (iii) the appearance of a remanent moment, and (iv) the relaxation onset. In spite of all the outlined difficulties, almost all the data points fall on a unique curve, indicating that there is an experimentally well-defined field $H_p(T)$ at which flux penetration occurs. This means that remanence and relaxation appear as soon as the departure from the Meissner behavior is detected, within our experimental resolution. The scattering is more evident at low temperatures, where flux pinning is more effective, and thus the transition to the irreversible mixed state takes place in a more gradual way.

The temperature dependence of $H_p(T)$ displays an upward curvature, and there is no indication of saturation at the lowest temperatures; the shape of this curve does not agree with the predictions of the mean-field theories for the lower critical field; $H_p(T)$ cannot be described by the usual empirical dependences for $H_{c1}(T)$, that is, $H_{c1}\sim(1-t^2)$ [low temperature Ginzburg-Landau (GL) extension] or $H_{c1}\sim(1-t^4)$ (two-fluid model); $t\equiv T/T_c$ is the reduced temperature. Nevertheless, it can be satisfactorily described by a law $H_p(T)=H_p(0)(1-t)^2$, taking as T_c the temperature at which the low-field diamagnetic onset occurs (see Table I) and fitting $H_p(0)$. The solid line in Fig. 8 corresponds to this fit for all different sets of experimental data points $H_p(T)$; it provides $\mu_0 H_p(0)\approx0.1$ T. It is worth mentioning that this fit does not depend on whether we include the point corresponding to $T=T_c$; that is, the obtained $H_p(T)$ function extrapolates to $H_p=0$ for $T=T_c$, in a natural way.

Similar dependences $H_p(T)\sim(1-t)^n$, $n\approx2$, have been obtained for all the measured single crystals. In Fig. 9(a) we summarize the $H_p(t)$ values obtained for all crystals by using the B_{res} criterion. It may be appreciated that the $H_p(T)$ values are significantly different; two groups can be established: those with thickness $\varepsilon\leq30$ μm (that is, Pr1, Nd1, and Nd2) display high penetration field values, $\mu_0 H_p(0)\approx0.1$ T, while thicker crystals display much lower $\mu_0 H_p(T)$ values. Several possible explanations of this fact can be proposed: first, crystals with extreme geometry have higher H_p values because of the higher demagnetizing factor, $N\approx1$; small inaccuracies in

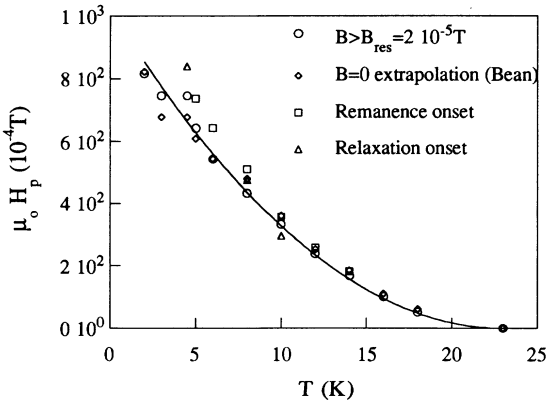

FIG. 8 Temperature dependence of the first flux-penetration field for crystal Nd2. The different symbols stand for the use of a criterion $B_{res}=2\times10^{-5}$ T, the extrapolation to zero of the square root of B, the appearance of a remanent moment, and the relaxation onset. The solid line is a fit of all data sets to $H_p\sim(1-t)^2$.

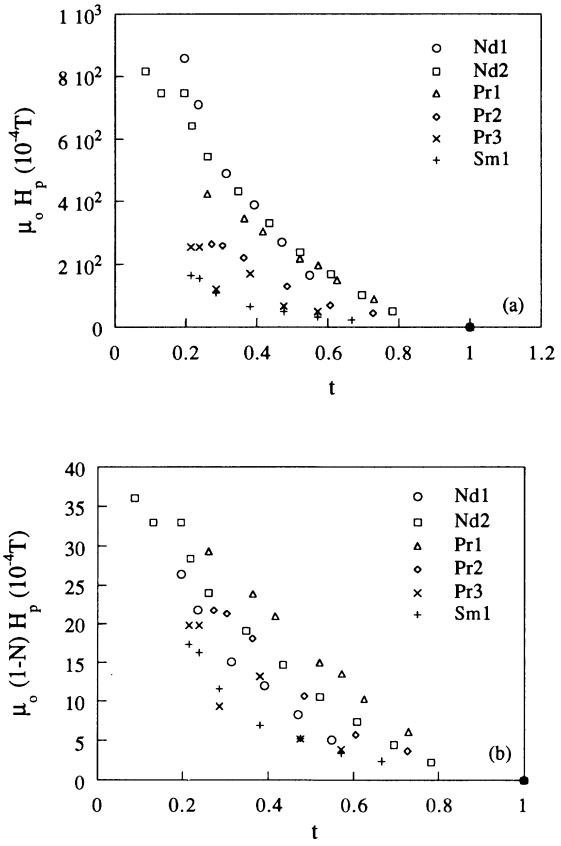

FIG. 9. Dependence on the reduced temperature $t=T/T_c$ of (a) the first flux-penetration field along the direction $\mathbf{H}\|\mathbf{c}$, in several analyzed single crystals (see Table I), as a function of the reduced temperature; and (b) the applied field $\mathbf{H_a}\|\mathbf{c}$ at which flux penetration appears.

the estimates of N would thus induce large differences in H_p, more pronounced in thinner crystals. Second, thicker crystals are likely to be inhomogeneous,[25] and this fact might provide lower H_p values. Due to the correlation between ε and N, we may not distinguish between both explanations. Besides, the high values of $1/(1-N)$ make the applied fields $(1-N)H_p$ to differ only in several Gauss, as appreciated in Fig. 9(b). Alternatively, it might be thought that, for a constant resolution of the magnetometer, deviation from the linearity by using a $B_{\rm res}$ threshold would provide lower H_p values in bigger crystals, as the measured signal is larger; however, we have not observed a clear trend in this sense when comparing the data obtained for the six analyzed crystals.

Let us go back to the temperature dependence of $H_p(T)$ and its meaning. As mentioned above, the curve $H_p(T)$ is not linear near T_c and does not saturate at low temperatures. These observations, in sharp contrast with regard to the predictions for $H_{c1}(T)$ in a mean-field theory, imply that $H_p(T)$ may not be directly identified with the lower critical field. An upward curvature of $H_{c1}(T)$ was predicted for superconductor-insulator layers in Ref. 26. However, in this situation one should expect to observe similar $H_p(T)$ values for crystals having similar critical temperatures. Data in Fig. 9(a) reveal that at low temperature ($t \approx 0.2$) the H_p values may differ within a factor as large as 5, thus suggesting that the upwards curvature is not due to the multilayered structure of the material.

Two possible reasons, deeply discussed above, stand out for $H_p(T)$ to be different from $H_{c1}(T)$: bulk pinning[20] and surface barriers.[2,4,27] Let us analyze them. Brandt and co-workers[20] have shown, assuming a critical state model with a field-independent critical current, that flux penetration for $\mathbf{H_a}$ applied perpendicular to a thin slab of thickness ε, should take place at a field $H_p \sim 0.1 J_c \varepsilon$. $H_p(T)$ would thus display the same upwards curvature reported for $J_c(T,H)$ in this temperature range.[19] Values of $J_c \leq 10^9$ A/m^2 have been reported from inductive measurements[19] on LCCO single crystals similar to those analyzed in this work; these low critical current values would provide penetration fields lower than those shown in Fig. 9(a). Furthermore, according to Ref. 20 higher H_p values should be found for thicker samples, in remarkable contrast with the behavior displayed by our crystals. Consequently, this explanation should be disregarded.

The absence of saturation of the first penetration field at low temperatures in several HTSC single crystals has been discussed in terms of the existence of surface barriers in the samples.[2,4,27] The presence of surface barriers in our single crystals might explain the observed correlation between $H_p(T)$ and the crystals thickness: defective surfaces parallel to the **c** axis are more likely to exist in thicker samples, and consequently surface barriers could become less effective. It is interesting to mention, however, that the shape of the hysteresis cycles appears to deny an important effect of surface barriers in these materials;[19] indeed, the increasing and decreasing field branches are symmetrical at any temperature, whereas theory predicts that the decreasing field branch must be flat and lie close to $M=0$ (Refs. 4, 5, and 27) when bulk pinning is weak, as it appears to be in LCCO crystals.[19] Moreover, it has been shown above (Fig. 7) that thermally activated processes are mainly related to bulk pinning; this fact implies that surface barriers have become unimportant when $H \approx H_p(T)$.

In either case, the lowest $H_p(T)$ values in Fig. 9(a) may be considered an upper limit for $H_{c1}(T)$ in these materials. We would therefore have $\mu_0 H_{c1}(0) \leq 0.02$ T and $\lambda_{ab}(0) \geq 1500$ Å; these values are remarkably similar to those reported for HTSC. Using $\mu_0 H_{c2}(0) \approx 6$ T (Ref. 28), a value of $\kappa \sim 20$ would be obtained for the Ginzburg-Landau parameter. Though this value is much higher than unity, it is notably lower than those estimated for HTSC ($\kappa \sim 100$); the reason for this difference stems from the large coherence length values in the LCCO system [$\xi_{ab}(0) \sim 80$ Å)] or, equivalently, from the low upper critical field values in this direction.

B. H‖ab

Figure 10 shows the anisotropic low-field dc susceptibility ($\mu_0 H_a \sim 10^{-4}$ T), measured after a ZFC process in crystal Pr1. Two features may be noted: (i) the transition in the $\mathbf{H_a}\|\mathbf{ab}$ direction is much broader than in the $\mathbf{H_a}\|\mathbf{c}$ direction; in the former case $\chi(T)$ does not reach saturation nor complete screening at the lowest measured temperatures. And (ii) the diamagnetic onset takes place at the same temperature in both directions. Similar behavior has been observed for all the analyzed samples (Pr1, Nd1, Nd2, Pr4).

The transition width in the $\mathbf{H_a}\|\mathbf{ab}$ direction might be simply related to size effects: in this geometry, the field is applied parallel to the largest surface of the crystals, and thus the cross section perpendicular to the field—where the screening currents flow— is very small, of the order of the thickness ε times the effective radius a. If the penetration depth along the **c** axis direction λ_c may not be ignored with regard to the crystal thickness ε, magnetic flux is never totally excluded from the sample, and the diamagnetic transition will not show complete saturation at low temperature; moreover, as $\lambda_c(T)$ increases ap-

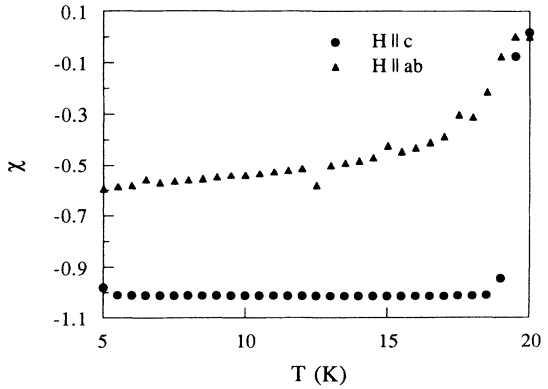

FIG. 10. Anisotropic low-field ZFC susceptibility ($\mu_0 H_a \sim 10^{-4}$ T) in crystal Pr1.

proaching T_c, $\chi(T)$ will reflect the temperature dependence of the screened volume, which decreases as T increases. In fact, we have observed that crystals with thickness similar to Pr1 ($\varepsilon \leq 30$ μm, as Nd1 and Nd2) display similar low $|\chi(T)|$ values, whereas $\chi(T)$ in thicker crystals (as Pr4, with $\varepsilon \sim 60$ μm) approaches total screening at low temperatures.

One way to assess the importance of size effects is by analyzing the linearity of the first magnetization curve; in the Meissner state, magnetization must be linear with H, even though $|\chi(T)| < 1$. This linear behavior is observed at the lowest fields in Fig. 11, which displays the first magnetization curves along the **H**||**ab** direction in crystal Pr4. Besides, the low-field ($\mu_0 H_a \sim 10^{-4}$ T) susceptibility curves $\chi(T)$ are coincident at low temperature. These experimental results support the explanation of the broad $\chi(T)$ transition as due to size effects in the Meissner state. Furthermore, the slope $dM/dH_a|_{T=ct}$ shows a trend to saturation at the lowest measured temperatures ($T \sim 2$ K). The penetration depth λ_c may thus be estimated from the $\chi(T)$ value, which must reflect the existence of a temperature-dependent screened volume V_{SC}:

$$\chi(T) = -\frac{V_{SC}(T)}{V} \approx -\frac{\varepsilon - 2\lambda_c(T)}{\varepsilon} .$$

A value $\chi(T) \approx -0.6$ (corresponding to $T = 5$ K in crystal Pr1) provides thus $\lambda_c \sim 0.2\varepsilon \sim 6$ μm.

Let us analyze more precisely the first magnetization curves displayed in Fig. 11; the demagnetizing field in the **H**||**ab** direction may be ignored, so that $H_a \approx H$. The first flux-penetration field $H_p(T)$ can be obtained by using the same procedure carried out for the **H**||**c** direction. We define the deviation from linearity by $\Delta M \equiv M - \chi_M H$; here χ_M is the Meissner susceptibility, now temperature dependent, since the $\chi(T)$ curve does not saturate; consequently, $\chi_M(T)$ must be determined at each temperature, from the linear $M(H)$ behavior at the lowest applied fields. Figure 12 shows ΔM as a function of the applied field; the first penetration field obtained from these data is

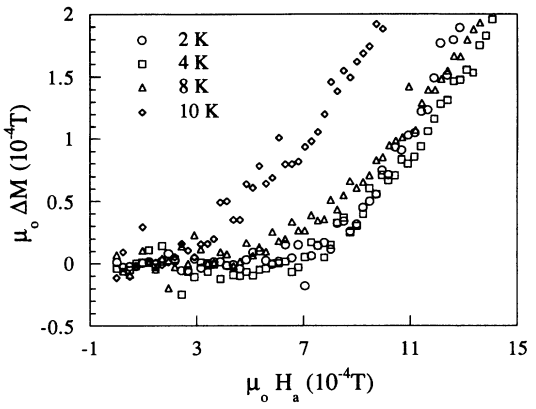

FIG. 12. Deviation from linearity ΔM, as a function of the applied field H_a, obtained from data in Fig. 11.

shown in Fig. 13. A remarkable difference may be appreciated, with regard to the temperature dependence of $H_p(T)$ in the **H**||**c** direction; data in Fig. 13 show that $H_p(T)$ saturates at low temperatures and does not display any anomalous upwards. Consequently, $H_p(T)$ behaves as expected for $H_{c1}(T)$. Assuming that $H_p(T) \approx H_{c1}(T) = (\Phi_0/4\pi\lambda_{ab}\lambda_c)\ln\kappa$, the extrapolated value $H_p(0)$ would provide a penetration depth $\lambda_c \sim 5$ μm; in this estimation use has been made of $\lambda_{ab}(0) \sim 1500$ Å, corresponding to $\mu_0 H_{c1}^c \approx 0.02$ T (see the above discussion concerning H_{c1}^c); the obtained value for λ_c is in agreement with that estimated from the low field $\chi(T)$ curves in the linear region [$H < H_p(T)$]. These observations allow us to identify $H_p(T)$ with $H_{c1}^{ab}(T)$. The solid line in Fig. 13 is a fit to the H_{c1} temperature dependence expected in the two-fluid model, $H_{c1}(T) \sim (1 - t^4)$, with $\mu_0 H_p(0) \sim 5 \times 10^{-4}$ T; the dashed line corresponds to a fit to the GL theory extended at low temperatures, $H_{c1}(T) \sim (1 - t^2)$; clearly, this latter fit is less satisfactory than the former one. In both cases we have left T_c as a

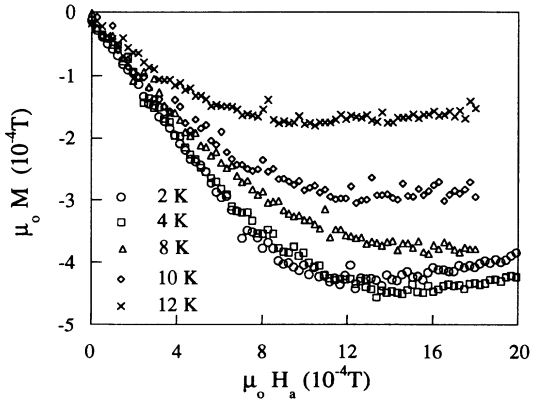

FIG. 11. First magnetization curves in crystal Pr4, in the $\mathbf{H_a}$||**ab** direction. The saturation in the first penetration field may be appreciated by the fact that the $M(H)$ curves at the lowest temperatures coincide.

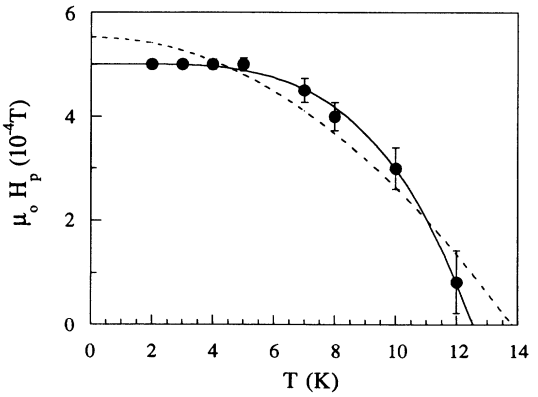

FIG. 13. Temperature dependence of the first penetration field along the **ab** planes in crystal Pr4. The solid (dashed) line is a fit to the temperature dependence expected in a two-fluid (GL extended to low temperatures) model.

fitting parameter, as $H_p(T)$ becomes vanishingly small near the diamagnetic onset temperature (Table I). As shown in Fig. 12, at temperatures $T \geq 12$ K the deviation from linearity in $M(H_a)$ is apparent in the experimental data even at the lowest measured fields, showing that flux penetrates the crystal at fields as low as $\mu_0 H_a \sim 10^{-5}$ T. This behavior which translates in Fig. 13 into a $H_p(T)$ curve extrapolating to zero at a temperature $T \sim 12.5$ K, below the diamagnetic onset measured at $\mu_0 H_a \approx 10^{-4}$ T (which coincides for the applied fields along the two main crystallographic directions, $T_c = 18$ K) is unexpected. In a mean-field theory built for Josephson-coupled layered superconductors, Clem, Coffey, and Hao[29] showed that the shape of the $H_{c1}^{ab}(T)$ curve is different from that derived for the Abrikosov model, but H_{c1} goes to zero at $T = T_c$ in both models. This prediction is in sharp contrast with our result. An alternative viewpoint may be proposed on the basis of the importance of magnetic fluctuations, which are known to be important in HTSC and also in LCCO.[28] Recently, Brawner *et al.*[30] have reported high-resolution $H_{c1}(T)$ measurements in $Bi_{2-x}Sr_2Ca_2Cu_2O_{10}$ (BSCCO) single crystals, with **H**||**c**. These experiments have shown that $H_{c1}^{c}(T)$ falls sharply to zero at a temperature T_{c0} well below the temperatures T_R where $H_{c1}^{c}(T)$ extrapolates to zero; this interesting behavior has been interpreted by Blatter, Ivlev, and Nordberg[31] in terms of a fluctuation-dominated regime, resulting in a reduced vortex line energy which vanishes at $T \approx T_{c0} < T_R$. To our knowledge, the full theory has not been developed yet for parallel fields, but our data suggest that fluctuations of the vortex lines could also play an important role in this case, and thus $H_{c1}^{ab}(T)$ could be also expected to vanish below $T_R \approx T_c = 18$ K. At this point, it may be useful to estimate $T_R - T_{c0}$ for LCCO (**H**||**c**) by using typical parameters ($T_c \approx 20$ K, $\lambda \approx 1500$ Å, $s = 6$ Å). We obtain $T_R - T_{c0} \approx 0.4$ K. This small temperature shift is well below our experimental resolution in the $H_{c1}^{c}(T)$ determination (Figs. 8 and 9). To what extent vortex fluctuations for **H**||**ab** should be more important remains an open question.

Once $H_{c1}^{ab}(T)$ has been evaluated, estimates of the anisotropy in electron-doped copper oxides can be obtained, since $H_{c1}^{c}/H_{c1}^{ab} \approx \lambda_c/\lambda_{ab} = \Gamma^{1/2}$. A concluding result is hindered by the difficulties in interpreting the meaning of the penetration field along the c-axis direction. A value of $\mu_0 H_{c1}^{c} \approx 0.02$ T, corresponding to the upper limit estimated in (a) provides $\Gamma \approx 1600$, lying closer to the estimates reported by Uji, Shimizu, and Aoki;[32] in fact, the Γ value in Ref. 32 was obtained from the dependence of resistivity on the orientation between the crystal and the applied field, which is assumed to be a reliable method to estimate the anisotropy in highly anisotropic systems. On the other hand, a value of $\Gamma \approx 1600$ would also be consistent with the observation of field-induced diamagnetic fluctuations of a two-dimensional nature.[28] According to this, the LCCO superconductors are much more anisotropic than Y-Ba-Cu-O ($\Gamma \approx 55$, Ref. 33), though not as extreme as BSCCO ($\Gamma \geq 3000$, Ref. 34).

In summary, the first magnetization curves along the two main crystallographic directions have allowed us to obtain the first penetration fields in both directions, 0.02 T $\leq \mu_0 H_p^{c}(0) \leq 0.1$ T (sample dependent) and $\mu_0 H_p^{ab}(0) \approx 0.5$ mT. The identification $H_{c1}^{ab} = H_p^{ab}$ appears to be appropriate. Unfortunately, the meaning of $H_p^{c}(T)$, displaying an upwards curvature down to the lowest measured temperatures, is masked by pinning, surface barriers, and shape effects; hence, the identification of $H_p^{c}(T)$ with $H_{c1}^{c}(T)$ cannot be safely assumed. Consequently, we could not obtain concluding values for the anisotropy ratio and the Ginzburg-Landau parameter in electron-doped superconducting copper oxides and only some limiting values can be drawn. The most likely values for the different intrinsic quantities determines in this work would be $H_{c1}^{c}(T) \leq 0.02$ T, $\lambda_{ab}(0) \geq 1500$ Å, $\Gamma \approx 1600$, $\kappa \approx 20$.

ACKNOWLEDGMENTS

We acknowledge many helpful discussions with Professor X. Obradors. This work was supported by the CICYT-MIDAS (MAT91-0742) and DGICYT (PB8971) projects from the Spanish Government. One of us (L.F.) would like to thank the Spanish Ministerio de Educación y Ciencia for support.

[1] C. P. Bean and J. D. Livingston, Phys. Rev. Lett. **12**, 14 (1964).
[2] M. Konczykowski, L. Burlachkov, Y. Yeshurun, and F. Holtzberg, Phys. Rev. B **43**, 13 707 (1991); L. Burlachkov, M. Konczykowski, Y. Yeshurun, and F. Holtzberg, J. Appl. Phys. **70**, 5759 (1991).
[3] B. V. Petukhov and V. R. Chechetkin, Zh. Eksp. Teor. Fiz. **65**, 1653 (1974) [Sov. Phys. JETP **38**, 827 (1974)]; V. P. Galaïko, Zh. Eksp. Teor. Fiz. **50**, 1322 (1966) [Sov. Phys. JETP **23**, 878 (1966)].
[4] V. N. Kopylov, A. E. Koshelev, I. F. Schegolev, and T. G. Togonidze, Physica C **170**, 291 (1990).
[5] A. M. Campbell and J. E. Evetts, Adv. Phys. **22**, 199 (1972).
[6] J. A. Cape, Phys. Rev. **179**, 485 (1969); J. A. Cape and J. M. Zimmerman, *ibid.* **153**, 416 (1967).
[7] H. P. Wiesinger, F. M. Sauerzopf, and H. W. Weber, Physica C **203**, 121 (1992).
[8] M. Konczykowski *et al.*, Phys. Rev. B **44**, 7167 (1991).
[9] C. C. Almasan, S. H. Han, E. A. Early, B. W. Lee, C. L. Seaman, and M. B. Maple, Phys. Rev. B **45**, 1056 (1992).
[10] G. Balakrishnan, C. K. Subramaniam, D. McK.Paul, S. Piñol, and R. Vijayaraghavan, Physica C **177**, 310 (1991).
[11] G. M. Luke *et al.*, Phys. Rev. B **42**, 7981 (1990).
[12] S. Piñol, J. Fontcuberta, C. Miravitlles, and D. McK.Paul, Physica C **165**, 465 (1990).
[13] U. Welp *et al.* (unpublished).
[14] L. D. Landau and E. M. Lifshitz, *Electrodynamics of Continuous Media* (Pergamon, New York, 1960).
[15] J. C. Martínez, J. J. Préjean, J. Karpinski, E. Kaldis, and P. Bordet, Solid State Commun. **75**, 315 (1990).
[16] A. Umezawa, G. W. Crabtree, J. Z. Liu, T. J. Morán, S. K. Malik, L. H. Núñez, W. K. Kwok, and C. H. Sowers, Phys. Rev. B **38**, 2843 (1988).

[17]C. P. Bean, Rev. Mod. Phys. **2**, 31 (1964).
[18]L. Fàbrega, B. Martínez, J. Fontcuberta, and S. Piñol, Phys. Rev. B **48**, 13 840 (1993).
[19]L. Fàbrega, J. Fontcuberta, and S. Piñol, Physica C **224**, 99 (1994).
[20]E. H. Brandt, Rev. B **46**, 8628 (1992); E. H. Brandt, M. V. Indenbom, and A. Forkl, Europhys. Lett. **22**, 735 (1993).
[21]M. Xu, Phys. Rev. B **44**, 2713 (1991).
[22]G. RaviKumar and P. Chaddah, Phys. Rev. B **39**, 4704 (1989); M. Xu, A. Umezawa, and G. W. Crabtree, *ibid.* **46**, 11 928 (1992).
[23]P. W. Anderson and Y. B. Kim, Rev. Mod. Phys. **36**, 39 (1964).
[24]A. E. Koshelev, Physica C **185-189**, 2435 (1991); **191**, 219 (1992).
[25]It has been recently observed that a Ce gradient along the c-axis direction may exist in thick crystals grown by the self-flux method. See, for instance, A. R. Drews, M. S. Osofsky, H. A. Hoff, J. L. Peng, Z. Y. Li, and R. L. Greene, Physica C **200**, 122 (1992); S. Piñol *et al.* (unpublished).
[26]T. Koyama, N. Takezawa, and M. Tachiki, Physica C **168**, 69 (1990).
[27]L. Burlachkov, Phys. Rev. B **47**, 8056 (1993).
[28]L. Fàbrega, J. Fontcuberta, X. Obradors, U. Welp, and G. W. Crabtree, Europhys. Lett. **24**, 595 (1993).
[29]J. R. Clem, M. W. Coffey, and Z. Hao, Phys. Rev. B **44**, 2732 (1991).
[30]D. A. Brawner, A. Schilling, H. R. Ott, R. J. Haug, K. Ploog, and K. von Klitzing, Phys. Rev. Lett. **71**, 785 (1993).
[31]G. Blatter, B. Ivlev, and H. Nordborg, Phys. Rev. B **48**, 10 448 (1993).
[32]S. Uji, T. Shimizu, and H. Aoki, Physica C **185-189**, 1309 (1991).
[33]U. Welp, W. K. Kwok, G. W. Crabtree, K. G. Vandervoort, and J. Z. Liu, Phys. Rev. Lett. **62**, 1908 (1989).
[34]J. C. Martínez, S. H. Brongersma, A. E. Koshelev, B. Ivlev, P. H. Kes, R. P. Griessen, D. G. de Groot, Z. Tarnavsli, and A. A. Menovski, Phys. Rev. Lett. **69**, 2276 (1992).